Structural and functional models for [NiFe] hydrogenase

Angamuthu, R.

Citation

Angamuthu, R. (2009, October 14). *Structural and functional models for [NiFe] hydrogenase*. Retrieved from https://hdl.handle.net/1887/14052

7

A Molecular Cage of Ni(II) and Cu(I) Resembling the Active site of Ni-Containing Enzymes†

Abstract. A new mononuclear low-spin nickel(II) dithiolato complex, [Ni(mpsms)$_2$] reacts with copper iodide to form the hetero-octanuclear cluster [{Ni(mpsms)$_2$}$_2$(CuI)$_6$]. The precursor complex [Ni(mpsms)$_2$] and the cluster are fully characterized by physicochemical methods. The molecular structure of the cluster is determined by X-ray crystallography, which has two distorted square-planar NiS$_4$, four trigonal-planar CuI$_2$S and two tetrahedral CuI$_2$S$_2$ sites; the tetrahedrally distorted NiS$_4$ units resemble the nickel centre of the [NiFe] hydrogenase and the Ni–S–Cu–I cage structure is compared with the bifunctional enzyme carbon monoxide dehydrogenase/acetyl-coenzyme A synthase (CODH/ACS). Furthermore, novel anagostic Ni···H interactions are observed in the X-ray crystal structure of the molecular cage and have been confirmed to pertain in the solution employing variable temperature ^{1}H NMR spectroscopic studies.

---

† This chapter is based on: R. Angamuthu, L. L. Gelauff, M. A. Siegler, A. L. Spek. and E. Bouwman, *Chem. Commun.*, **2009**, 2700-2702.

7.1. Introduction

Nickel thiolato complexes, including (hetero-)multinuclear [NiFe], [NiCu], [NiZn] and [NiNi] units, are of interest in the context of their rich redox chemistry[1,2] and structural diversity in supramolecular architectures,[3] as is discussed in Chapter 6. Furthermore, they are important as synthetic models[1,4-7] for environmentally and industrially significant enzymes like hydrogenases, superoxide dismutases and CODH/ACS. The focus of attention for this Chapter is to study the chemistry involving the synthesis and reactivity of nickel thiolate complexes in relation with the structure and function of active sites in nickel-containing enzymes.[1,4-7] The mononuclear [Ni(mpsms)$_2$] discussed in Chapter 4 has now been used in a reaction with CuI resulted in a molecular cage of Ni(II) and Cu(I) resembling the active site of Ni-containing enzymes such as [NiFe] hydrogenase and the A-cluster of the CODH/ACS. This Chapter reports on the formation and structural properties of the cluster [{Ni(mpsms)$_2$}$_2$(CuI)$_6$] having two distorted square-planar NiS$_4$, four trigonal-planar CuI$_2$S and two tetrahedral CuI$_2$S$_2$ sites. In addition, the anagostic interactions between the Ni(II) ions and the *ortho*-protons of the phenyl rings of the ligands are demonstrated using both X-ray crystallography and NMR spectroscopic techniques.

7.2. Results and Discussion

7.2.1. Synthesis

The reaction of Ni(acac)$_2$ with two equivalents of the thiouronium chloride salt of the ligand, in the presence of two equivalents of tetramethylammonium hydroxide led to an immediate colour change to deep brown and the new low-spin square-planar complex [Ni(mpsms)$_2$] was isolated as flocculent reddish-brown crystals in high yield. Equimolar solutions of Ni(mpsms)$_2$ in dichloromethane and copper(I) iodide in acetonitrile were mixed under argon and stirred for an hour to yield a dark brown precipitate. A saturated solution of this product in absolute ethanol was left for slow evaporation under argon atmosphere and dark brown crystals of [{Ni(mpsms)$_2$}$_2$(CuI)$_6$] were formed over several days. The molecular structure of [{Ni(mpsms)$_2$}$_2$(CuI)$_6$], which has been determined by single crystal X-ray diffraction, shows a spectacular cage structure formed by the thiolate sulfurs and copper iodide moieties.

7.2.2. Molecular Structure of [{Ni(mpsms)$_2$}$_2$(CuI)$_6$]

The molecular structure of [{Ni(mpsms)$_2$}$_2$(CuI)$_6$] is shown in Fig. 7.1 and important bond lengths and angles are provided in Table 7.1. The asymmetric unit of [{Ni(mpsms)$_2$}$_2$(CuI)$_6$] contains one crystallographically independent ordered molecule (Fig. 7.1), and no solvent molecules are found in the crystal lattice. The two Ni(II) centers are in slightly distorted square-planar environments with two thiolate donors and two thioether sulfurs in enforced *cis* positions. The Ni–S_{thiolate} distances [2.1641(14)-2.1788(14) Å] are slightly shorter than the Ni-$S_{\text{thioether}}$ distances [2.1856(15)-2.2028(16) Å], as expected. The nickel centers have a slight tetrahedral distortion with a dihedral angle of 3.58(8)° for Ni1 (between the triangular planes S6Ni1S9 and S16Ni1S19) and 9.13(8)° for Ni1A (between the triangular planes S6ANi1S9A and S16ANi1S19A).

Table 7.1. Selected bond lengths (Å) and angles (°) of $[\{Ni(mpsms)_2\}_2(CuI)_6]$. Atoms that are labeled with and without 'A' are crystallographically independent.

Cu1⋯Cu1A	2.6032(10)	Cu2⋯Cu2A	4.0309(10)	Cu1⋯Cu3	5.3644(2)
Cu1⋯Cu2	3.9844(9)	Ni1⋯Ni1A	6.6421(9)	Ni1⋯Cu1	3.5495(9)
Ni1⋯Cu2	3.8655(9)	Ni1⋯Cu3	3.5982(10)	Ni1–S6	2.1641(14)
Ni1–S9	2.2028(16)	Ni1–S16	2.1757(15)	Ni1–S19	2.1932(14)
Cu1–S6	2.2925(14)	Cu2–S6	2.4417(15)	Cu1–I1	2.5955(8)
Cu1–I2	2.5271(8)	Cu2–I2A	2.6337(7)	Cu2–I3A	2.6296(7)
S6–Ni1–S9	92.17(6)	S9–Ni1–S19	90.04(6)	S16–Ni1–S19	92.08(6)
S6–Ni1–S16	85.82(6)	S6–Ni1–S19	176.89(6)	S9–Ni1–S16	176.47(6)
S6–Cu1–I1	109.11(4)	I1–Cu1–I2	124.21(3)	S6–Cu1–I2	126.61(4)
S6–Cu2–I2A	110.40(4)	I2A–Cu2–S16A	99.90(4)	I3A–Cu2–S16A	107.65(4)
S6–Cu2–I3A	98.61(4)	S6–Cu2–S16A	122.29(5)	I2A–Cu2–I3A	119.38(3)

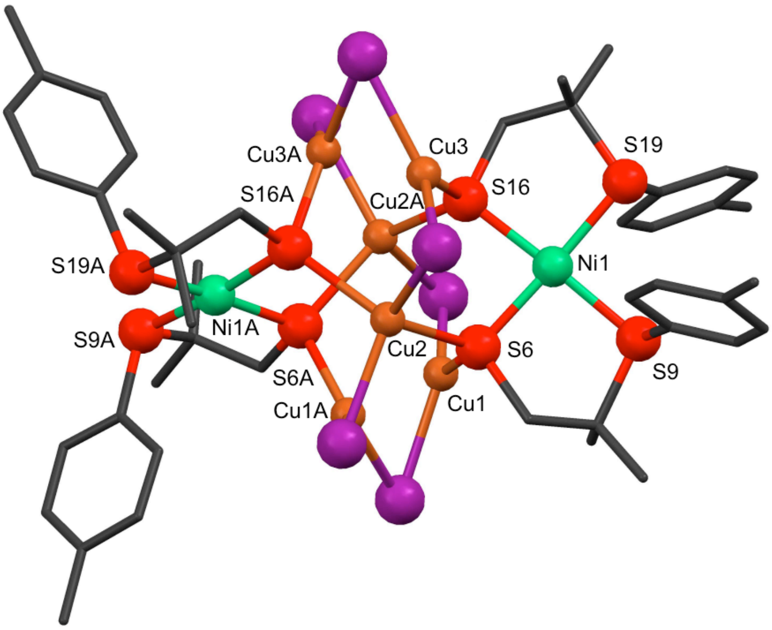

Fig. 7.1. Perspective view of $[\{Ni(mpsms)_2\}_2(CuI)_6]$. Ni, green; Cu, brown; S, red; I, violet; C, grey. Hydrogens are omitted for clarity.

The six copper iodide moieties are forming altogether a twelve membered Cu_6I_6 puckered-crown (Fig. 7.2) in which the six iodides are bridged between the copper ions in μ-fashion to form this crown. The two square-planar NiS_4 units are capping this crown from both sides utilizing their thiolate sulfurs to form $[\{Ni(mpsms)_2\}_2(CuI)_6]$; the dihedral angle defined by these two S_4 planes is 72.10(5)°. Each thiolate sulfur is bound to two copper(I) ions, of which one is in a trigonal-planar geometry and the other possesses tetrahedral geometry. The tetrahedral copper ions are shared between the two NiS_4 units by direct S–Cu–S bridging, while the trigonal-planar copper ions are shared through a S–Cu–I–Cu–S bridge. The four thiolate sulfurs and the six copper(I) iodide units together form a cage structure in the middle of the two NiS_4 units (Fig. 7.2).

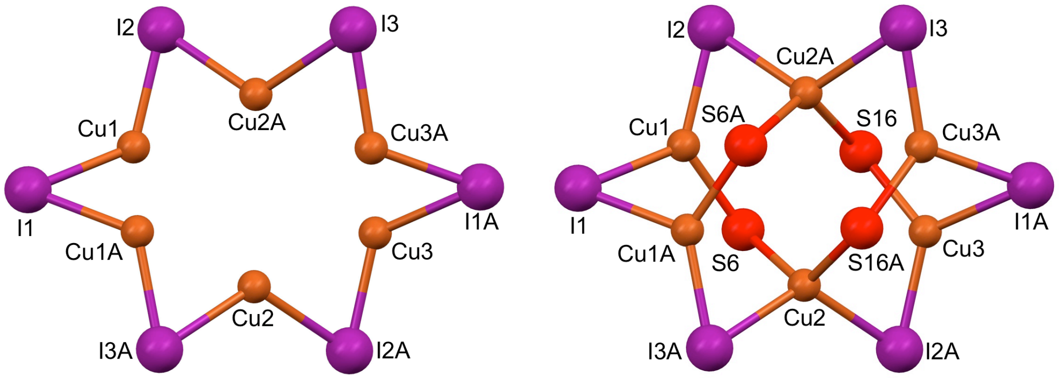

Fig. 7.2. Perspective views of the Cu_6I_6 puckered-crown (left) and $Cu_6I_6S_4$ cage (right) in [{Ni(mpsms)$_2$}$_2$(CuI)$_6$].

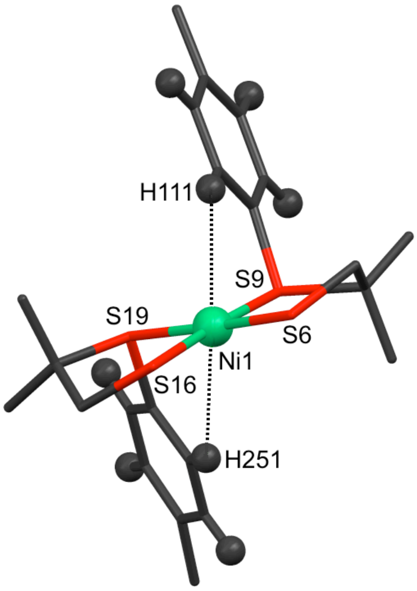

Fig. 7.3. Perspective view of one [Ni(mpsms)$_2$] part of [{Ni(mpsms)$_2$}$_2$(CuI)$_6$] with the atomic labeling of selected atoms. The nickel-to-hydrogen interactions are shown; only the hydrogens present in the 4–methylphenyl rings are shown for clarity. Ni1···H111, 2.739; Ni1···H251, 2.781; Ni1A···H152, 2.696; Ni1A···H212, 2.626 Å

The trigonal-planar copper ions, Cu1, Cu1A, Cu3 and Cu3A, are found in an I_2S coordination sphere of which one of the two iodide ions is bridged to a trigonal-planar copper ion, while the other iodide is bridged to a tetrahedral copper ion. The bond distances of iodide to copper vary due to this difference in bridging; the angles in the trigonal-planar CuI_2S moieties are not strictly 120°. Likewise, the angles in the tetrahedral CuI_2S_2 moieties also deviate from the ideal angle of 109.5°, and range from 98.61(4)° to 122.29(5)°.

An interesting interaction between the nickel(II) ion and the *ortho*–protons of the phenyl rings is observed, with distances of about 2.7 Å in both NiS_4 units of $[\{Ni(mpsms)_2\}_2(CuI)_6]$ (Fig. 7.3). Considering these interactions as bonding, the coordination geometry of the nickel ion could be described as pseudo-octahedral, in an $H_2N_2S_2$ chromophore, in which two *ortho*–protons occupy the axial sites of the octahedron.

7.2.3. Proton NMR Spectral Studies of $[\{Ni(mpsms)_2\}_2(CuI)_6]$

To investigate whether the structure of the $[\{Ni(mpsms)_2\}_2(CuI)_6]$ is retained in solution, ^1H NMR spectra of the complex have been recorded in CD_2Cl_2 solution at different temperatures ranging from 183 to 303 K. (Fig. 7.4). Even though there are four crystallographically distinct ligands are present in the complex, the ^1H NMR spectrum at room temperature shows only a single set of signals suggesting that the four ligands are equivalent in solution. Interestingly, upon cooling the sample to 263 K the signals start to broaden and eventually split into multiple sharp signals at 183 K.

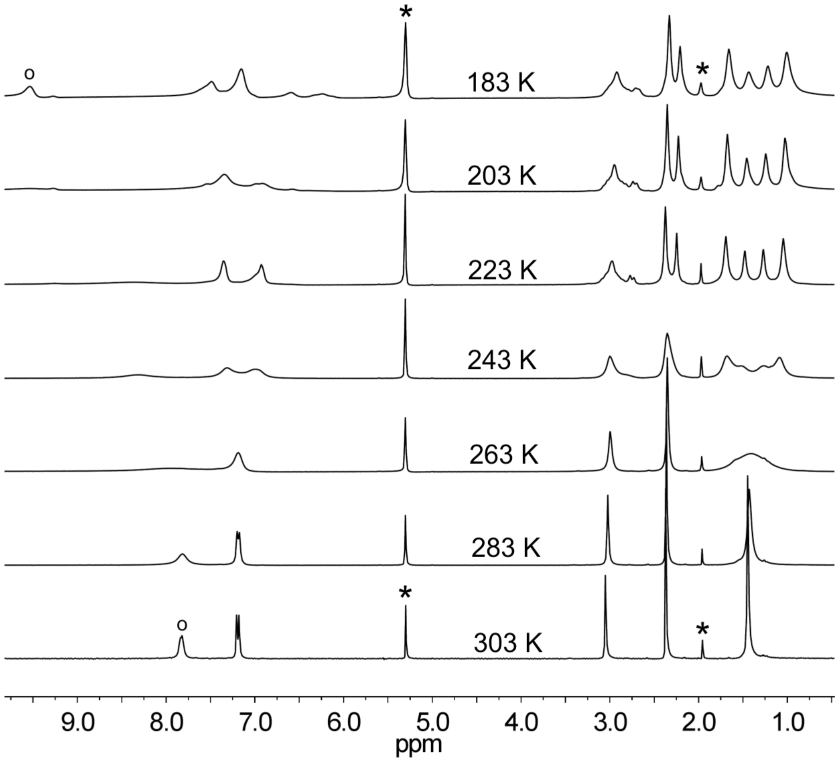

Fig. 7.4. ^1H NMR of $[\{Ni(mpsms)_2\}_2(CuI)_6]$ in CD_2Cl_2 recorded in different temperatures ranging between 183 and 303 K. ★, signals from CD_2Cl_2 (5.32 ppm) and acetone (2 ppm); ○, signals from the *ortho*–protons of the phenyl rings.

The fluxional axial and equatorial exchange of the dimethyl groups is slow or inhibited at low temperature; the singlet of the dimethyl protons (at 1.4 ppm) consequently splits into four sharp signals. Furthermore, the two aromatic resonances (at 7.1 and 7.8 ppm) are split in a number of resonances with different intensities; the protons involved in an interaction with the nickel ions are observed at δ 9.5 ppm upon cooling to 183 K. The downfield shift of these protons in the NMR spectrum, and the fact that they are pointing in the direction of the occupied d_{z^2} orbital of the nickel(II) ions (Fig. 7.3) at a distance of about 2.7 Å on average in the crystal structure, suggest that these interactions should be considered as anagostic or hydrogen bonding.[8-10]

7.2.4. Redox Properties of [{Ni(mpsms)$_2$}$_2$(CuI)$_6$]

The cyclic voltammogram of the [NiCu] cluster in a dichloromethane solution shows a number of irreversible oxidation processes (–0.273 V, –0.180 V, -0.076 V vs Ag/AgCl) and a single irreversible reduction process (–0.914 V) which are difficult to assign unequivocally due to the presence of the large number of redox non-innocent partners available in the multinuclear structure of [{Ni(mpsms)$_2$}$_2$(CuI)$_6$] (Fig. 7.5).

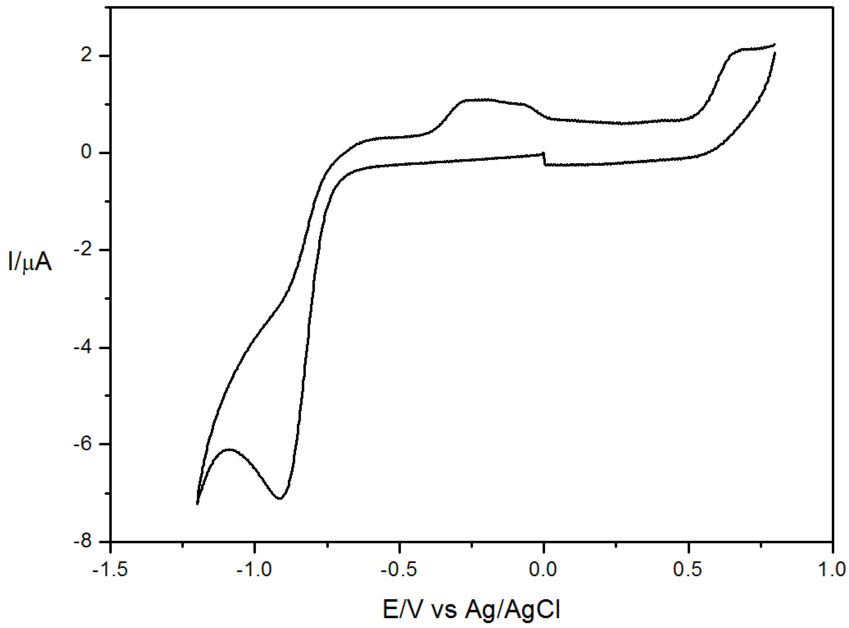

Fig. 7.5. Cyclic voltammogram of 0.5 mM solution of [{Ni(mpsms)$_2$}$_2$(CuI)$_6$] in CH_2Cl_2 containing 0.05 M $(NBu_4)PF_6$. Scan rate 100 mV s^{-1}. Static glassy carbon disc working electrode and Pt wire counter electrode used with Ag/AgCl reference electrode.

7.2.5. Relevance to the Ni-containing Enzymes

The presence of the 4-methylphenyl ring bound to the thioether sulfur paves the way to exhibit the attraction between the *ortho*–protons of the phenyl ring and the low-spin Ni(II) ion, as identified in the crystal structure and NMR spectroscopy (Fig. 7.3 and

Fig. 7.4). It appears that the cluster [{Ni(mpsms)$_2$}$_2$(CuI)$_6$] is the first compound with an NiS$_4$ coordination displaying the aforesaid nickel to proton anagostic interactions.

The tetrahedrally distorted NiS$_4$ coordination spheres of Ni1 and Ni1A in [{Ni(mpsms)$_2$}$_2$(CuI)$_6$] resemble the nickel centre of the "EPR silent active form" (Ni-SI$_a$) of [NiFe] hydrogenase with an Ni^{II}Fe^{II} electronic configuration that is the starting point of the catalytic cycle of the enzymatic action; protonation of this form generates the Ni-SI$_b$ form which then turns into Ni-R state upon hydrogenation.[11-14] Development of model complexes with this kind of Ni···H interaction may help to better understand the mechanistic insights of the [NiFe] hydrogenase and further to obtain improved structural and functional mimics. Furthermore, the Ni–μ_3–S–Cu motifs forming the cage in [{Ni(mpsms)$_2$}$_2$(CuI)$_6$] resemble the A-cluster of the CODH/ACS with a low-spin square-planar nickel (Ni$_d$) and bridging μ_3–thiolates connecting the tetrahedral copper (M$_p$).

7.3. Conclusions

In summary, a novel molecular cage of hetero-octanuclear nickel(II) copper(I) cluster, [{Ni(mpsms)$_2$}$_2$(CuI)$_6$] has been isolated in good yield by the reaction of the low-spin square-planar NiS$_4$ complex Ni(mpsms)$_2$ with CuI and has been characterized using single-crystal X-ray diffraction, NMR and electrochemistry techniques. The anagostic interactions between the nickel and aromatic *ortho*-protons have been demonstrated by the variable temperature NMR studies also to pertain in solution.

7.4. Experimental Procedures

7.4.1. General

Synthesis of the ligand precursor TU-mpsms and the mononuclear nickel complex [Ni(mpsms)$_2$] are described in Chapters **2** and **4**, respectively, along with the characterizations.

7.4.2. Synthesis of [Ni(mpsms)$_2$(CuI)$_6$]

A solution of CuI (191 mg, 1 mmol) in 10 ml acetonitrile was added to a solution of [Ni(L)$_2$] (483 mg, 1 mmol) in 10 ml chloroform and the mixture was stirred for an hour. After evaporation of the solvent, the product was recrystallized by the slow evaporation of an ethanolic solution in an argon atmosphere. Dark-brown crystals suitable for X-ray diffraction were obtained over a few days. [Ni(mpsms)$_2$(CuI)$_6$] was reproduced in bulk by the reaction between one equivalent of complex [Ni(mpsms)$_2$] and three equivalents of CuI in acetonitrile as a brown powder (87%). **^{1}H NMR:** δ_H [300.13 MHz, CD$_2$Cl$_2$, 298 K]) 7.84 (bs, 8H, phenyl–*ortho*–*H*), 7.22 (d, 8H, phenyl–*meta*–*H*), 3.06 (s, 8H, –CH_2–S–), 2.38 (s, 12H, CH_3–Ph), 1.46 (s, 24H, –C(CH_3)$_2$–) **^{13}C NMR:** δ_C [75.47 MHz, CD$_2$Cl$_2$, 298 K] 143.52

(Ph-C4), 136.54 (Ph-C3), 131.18 (Ph-C2), 122.75 (Ph-C1), 64.35 (–*C*(CH_3)$_2$–), 49.27 (–*C*H_2–), 27.69 ((–C(*C*H_3)$_2$–), 21.94 (*C*H_3–Ph). **Elemental Analysis (%):** calculated for $C_{44}H_{60}Cu_6I_6Ni_2S_8\cdot3CHCl_3$, C 22.91, H 2.58, S 10.41, found, C 22.67, H 2.54, S 10.28

7.4.3. Crystallographic Data for [{Ni(mpsms)$_2$}$_2$(CuI)$_6$]

All reflection intensities were measured at 110(2) K using a Nonius KappaCCD diffractometer (rotating anode) with graphite-monochromated Mo *K*α radiation (λ = 0.71073 Å) under the program *COLLECT*.[15] The program *PEAKREF*[16] was used to refine the cell dimensions. Data reduction was done using the program *EVALCCD*.[17] The structure was solved with the program *DIRDIF08*[18] and was refined on F^2 with *SHELXL-97*.[19] Analytical absorption corrections based on crystal face-indexing were applied to the data using *SADABS*.[19] The temperature of the data collection was controlled using the system *OXFORD CRYOSTREAM 600* (manufactured by *OXFORD CRYOSYSTEMS*). The H-atoms were placed at calculated positions (*AFIX 23* or *AFIX 43* or *AFIX 137*) with isotropic displacement parameters having values 1.2 times *U*eq of the attached C atom. Geometry calculations were performed with the *PLATON* program.[20]

$C_{44}H_{60}Cu_6I_6Ni_2S_8$, Fw = 2105.46, dark brown needles, 0.04 × 0.07 × 0.24 mm^3, triclinic, *P*-1 (no. 2), a = 11.6566(5), b = 14.1559(4), c = 19.9857(7) Å, α = 86.088(1), β = 84.143(1), γ = 70.505(2) °, V = 3090.5(2) Å^3, Z = 2, D_x = 2.263 g cm^{-3}, μ = 5.915 mm^{-1}. 67305 Reflections were measured up to a resolution of $(\sin \theta/\lambda)_{\max}$ = 0.62 Å^{-1}. An absorption correction based on multiple measured reflections was applied (0.48–0.87 correction range). 12170 Reflections were unique (R_{int} = 0.063), of which 8494 were observed [$I > 2\sigma(I)$]. 607 Parameters were refined. $R1/wR2$ [$I > 2\sigma(I)$]: 0.0361/0.0553. $R1/wR2$ [all refl.]: 0.0742/0.0634. S = 1.022. Residual electron density between −0.90 and 0.98 eÅ^{-3}.

7.5. References

1. E. Bouwman and J. Reedijk, *Coord. Chem. Rev.*, 2005, **249**, 1555-1581.
2. V. Artero and M. Fontecave, *Coord. Chem. Rev.*, 2005, **249**, 1518-1535.
3. C. Zhang, S. Takada, M. Kölzer, T. Matsumoto and K. Tatsumi, *Angew. Chem.-Int. Edit. Engl.*, 2006, **45**, 3768-3772.
4. J. A. W. Verhagen, C. Tock, M. Lutz, A. L. Spek and E. Bouwman, *Eur. J. Inorg. Chem.*, 2006, 4800-4808.
5. J. A. W. Verhagen, M. Beretta, A. L. Spek and E. Bouwman, *Inorg. Chim. Acta*, 2004, **357**, 2687-2693.
6. J. A. W. Verhagen, M. Lutz, A. L. Spek and E. Bouwman, *Eur. J. Inorg. Chem.*, 2003, 3968-3974.
7. J. A. W. Verhagen, D. D. Ellis, M. Lutz, A. L. Spek and E. Bouwman, *J. Chem. Soc.-Dalton Trans.*, 2002, 1275-1280.
8. E. Bouwman, R. K. Henderson, A. K. Powell, J. Reedijk, W. J. J. Smeets, A. L. Spek, N. Veldman and S. Wocadlo, *J. Chem. Soc.-Dalton Trans.*, 1998, 3495-3499.
9. W. B. Yao, O. Eisenstein and R. H. Crabtree, *Inorg. Chim. Acta*, 1997, **254**, 105-111.
10. M. Brookhart, M. L. H. Green and G. Parkin, *Proc. Natl. Acad. Sci. U. S. A.*, 2007, **104**, 6908-6914.

11. A. L. DeLacey, V. M. Fernandez, M. Rousset and R. Cammack, *Chem. Rev.*, 2007, **107**, 4304-4330.
12. W. Lubitz, E. Reijerse and M. van Gastel, *Chem. Rev.*, 2007, **107**, 4331-4365.
13. P. E. M. Siegbahn, J. W. Tye and M. B. Hall, *Chem. Rev.*, 2007, **107**, 4414-4435.
14. P. Jayapal, M. Sundararajan, I. H. Hillier and N. A. Burton, *Phys. Chem. Chem. Phys.*, 2008, **10**, 4249-4257.
15. Nonius, Nonius BV., Delft, The Netherlands, 1999.
16. A. M. M. Schreurs, University of Utrecht, The Netherlands, 2005.
17. A. J. M. Duisenberg, L. M. J. Kroon-Batenburg and A. M. M. Schreurs, *J. Appl. Cryst.*, 2003, **36**, 220.
18. P. T. Beurskens, G. Beurskens, R. de Gelder, S. Garcia-Granda, R. O. Gould and J. M. M. Smiths, University of Nijmegen, The Netherlands, **2008**.
19. G. M. Sheldrick, *Acta Cryst.*, 2008, **A64**, 112.
20. A. L. Spek, *J. Appl. Cryst.*, 2003, **36**, 7.